Asian Journal of Probability and Statistics

Volume 26, Issue 12, Page 234-252, 2024; Article no.AJPAS.128079
ISSN: 2582-0230

One-sided Cusum Chart with V-mask for Weighted Weibull Distribution Parameter Shifts

Shei Baba Sayibu [a*], Sualihu Mohammed Muntaka [a] and Alhassan Mubarika [b]

[a] Department of Statistics, Faculty of Physical Sciences, University for Development Studies, Tamale, West Africa, Ghana.
[b] Department of Statistical Science, Tamale Technical University, Tamale, West Africa, Ghana.

Authors' contributions

This work was carried out in collaboration among all authors. All authors read and approved the final manuscript.

Article Information

DOI: https://doi.org/10.9734/ajpas/2024/v26i12695

Open Peer Review History:
This journal follows the Advanced Open Peer Review policy. Identity of the Reviewers, Editor(s) and additional Reviewers, peer review comments, different versions of the manuscript, comments of the editors, etc are available here: https://www.sdiarticle5.com/review-history/128079

Original Research Article

Received: 07/10/2024
Accepted: 14/12/2024
Published: 21/12/2024

Abstract

In our research, we have developed a cumulative sum control chart to identify changes in the parameter of the weighted Weibull distribution. This chart incorporates the V-mask technique and a sequential ratio test. Our analysis of the V-mask revealed that even minor shifts in the weighted Weibull distribution's parameters led to significant variations in the mask's angle, lead distance, and average run length. A change in the V-mask parameters has the following importance: it can lead to an increase in false alarms, decreased detection of true signals, change in process capability, indicates the need for process adjustments, increased security from regulatory bodies, impact on supply chain and customer relationships, and the need for re-training or re-

**Corresponding author: Email: b.shei@yahoo.com, sheibaba@uds.edu.gh;*

Cite as: *Sayibu, Shei Baba, Sualihu Mohammed Muntaka, and Alhassan Mubarika. 2024. "One-Sided Cusum Chart With V-Mask for Weighted Weibull Distribution Parameter Shifts". Asian Journal of Probability and Statistics 26 (12):234-52. https://doi.org/10.9734/ajpas/2024/v26i12695.*

certification. Finally, we applied the cumulative sum chart to real data from the Kabsad Scientific Hospital to illustrate the sensitivity of the proposed cumulative sum control chart. The V-mask plot showed a shift in the process mean of the dataset.

Keywords: Deviations; flexibility; inadequacy; sensitivity; and variability.

1 Introduction

Product quality features have recently received much attention from design engineers, production personnel, and consumers. It has increasingly become apparent that improving product quality can decrease the cost of production and increase consumer satisfaction, culminating in a high percentage of profits.

Control charts are used widely as a diagnostic tool for monitoring production and services to identify instability and circumstances that are unusual in the process. A defect of the traditional Shewhart control chart is its inadequacy in detecting a relatively small change in a process mean. This is largely the consequence of whether a process is judged out of control at a particular time depends only on the sample at that time and not on the history of the process (Devore, 2012). Cumulative sum (CUSUM) control charts are statistical process control tools used to monitor process mean shifts based on system samples at given intervals. The intervals could be hours, days, weeks, or months. It makes use of the cumulative sum of deviations from a given point. It is a powerful technique for monitoring and controlling processes, particularly when the shift is small compared to the process variability. The CUSUM chart plots the cumulative sum deviations from the target point for individual measurements or subgroup means. It indicates the accumulative information of previous and current samples. Given this reason, the CUSUM control charts are more effective than the Shewhart control charts in detecting small shifts in the process mean. The CUSUM control chart depends on the specification of a target value and a known or reliable variance estimate. This makes the CUSUM chart a better tool in process control management. The CUSUM chart is flexible, sensitive to small shifts, enhances quality control, and is easy to implement. It is good for monitoring processes with small shifts, improving process stability, and reducing false alarms in systems. The CUSUM charts are useful in manufacturing, chemical processing, finance, and healthcare systems management. A one-sided CUSUM chart is used to detect shifts in one direction, either right-side or left-side. It is particularly applied when only one type of shift is of interest or when the process is more sensitive to shifts in one direction. The one-sided CUSUM's importance includes but is not limited to tracking vital signs such as blood pressure, heart rate, or oxygen saturation. Evaluation of quality of care, such as patient satisfaction, readmission, or complication rates. Monitoring infection rates, and antibiotic resistance of hospital-acquired infections, detecting trends or anomalies in stock prices, trading volumes, or market indices; monitoring financial risk, like credit risk, market risk, or operational risk. In environment monitoring, it can be used to track pollutants such as particulate matter, ozone, or nitrogen dioxide; monitor water quality parameters such as PH, turbidity, or bacteria contamination; and detect changes in climate patterns, such as temperature, precipitation, or sea level rise. Other importance includes, monitoring supply chain performance, such as lead times, inventory levels, or shipping errors, detect anomalies in network traffic, system logs, or user behavior. The first CUSUM control chart was introduced by Page (1954) and has since been widely used in various industries for monitoring and controlling processes. Other published works on CUSUM included combined Shewhart-CUSUM quality control scheme (Lucas, 1982), cumulative sum control charting (Hawkins, 1993), statistical design of CUSUM charts (Woodall and Adams, 1993), exact results for Shewhart control charts with supplementary run rules (Champ and Woodall, 2001), one-sided CUSUM control chart for the Erlang-Truncated exponential distribution (Rao, 2013), one-sided cumulative sum control chart for monitoring shifts in the shape parameter of the Pareto distribution (Nasiru, 2016), one-sided cumulative sum control chart for monitoring shift in the scale parameter, delta of the new Weibull-Pareto distribution (Sayibu et al., 2017), unified sum control chart for monitoring shifts in the parameters of the Pareto distribution (Sayibu and Maahi, 2017), two-sided cumulative sum control chart for monitoring shifts in the shape parameter of the Pareto distribution (Sayibu and Luguterah, 2018), distribution-free CUSUM control charts using bootstrap-based control limits (Zhang and Woodall, 2019), how to use a CUSUM chart for process improvement (Doganaksov and Hahn, 2020), CUSUM analysis (Grigg and Farewell, 2020), CGR-CUSUM: a continuous time generalized rapid response cumulative sum (Xie and Goh, 2022), efficient Monitoring of a Parameter of Non-Normal Process Using a Robust Efficient Control Chart: A Comparative Study (Chaudhary et al., 2023), on efficient change point detection using a step cumulative sum control chart (Abass, 2023), efficient CUSUM control charts for monitoring the multivariate coefficient of variation (Hu et al., 2023), a robust CUSUM control chart for median absolute deviation based on

trimming and winsorization (Khalil et al., 2024), proper choice of location CUSUM control charts for different environments (Nazir et al., 2024), a new CUSUM control chart under uncertainty with applications I petroleum and meteorology (Aslam et al., 2024), and control charts in health care quality monitoring (Waqas et al., 2024) among others.

The rest of the study is organized as follows: section 2 discusses the sequential probability ratio test, and weighted Weibull distribution is covered under Section 3. The cumulative sum control chart is enumerated in Section 4, average run length is treated in Section 5, practical application is illustrated in Section 6 and Section 7 covers the conclusion.

2 Sequential Probability Ratio Test

The sequential probability ratio test (SPRT) is a statistical test used to determine whether a process or system is stable or unstable. The test is performed sequentially, with data points added one after the other. The test calculates the ratio of probabilities of the data under two hypotheses and the test statistic is the cumulative sum of the logarithms of the probability ratios. It includes the following steps: defining the null and alternative hypotheses and setting the significance level, (δ) and power $(1-\theta)$. The rest are, calculating the test statistic for each new data point and comparing the test statistic to the upper and lower boundaries. If the test statistic crosses the upper boundary, reject the null hypothesis, thus out of control. On the other hand, if the test statistic crosses the lower boundary; accept the null hypothesis which means the system is in control. If the test statistic remains within the limits, continue the sampling process. The SPRT is efficient, flexible, and powerful. By way of illustration, Wald's SPRT is widely used for determining between two alternative hypotheses, $H_0 : \rho = \rho_0$ and $H_1 : \rho = \rho_1$. Let $x_1, x_2, ..., x_n$ denote successive observations of a random variable X which are independent and identically distributed and follow the weighted Weibull distribution (WWD). If the probability of observing $x_1, x_2, ..., x_n$ is given by $P_i(n)$ when H_i is true $(i = 0,1)$. If the pdf of the random variable is $f_i(x)$ when H_i is true, then

$$P_i(n) = f_i(x_1), ..., f_i(x_n)$$

Given two constants A and B such that $A > 0$ and $B > 0$, Wald's sequential test of H_i against H_0 is given as follows. At the n^{th} sampling stage, the logarithm of the probability ratio is

$$\eta(n) = \log \frac{P_1(n)}{P_0(n)} = \log \frac{L(\rho_1; X_1, ..., X_n)}{L(\rho_0; X_1, ..., X_n)} > K ,$$

is calculated. The Wald's SPRT has the following nature

- If $\eta(n) \geq A$, then terminate the observation and accept H_i as true
- $\eta(n) < A$ then decide that H_0 is true and terminate the process
- $A < \eta(n) < B$, continue to collect more observations to obtain η_{n+1} .

The SPRT is optimal as it minimizes the average sample size before a decision can be made within all sequential tests which do not have larger error probabilities than the SPRT. Furthermore, the boundaries A and B can be determined with a very good approximation as

$$A = \log \frac{\theta}{1-\delta} \text{ and } B = \log \frac{1-\theta}{\delta} .$$

3 Weighted Weibull distribution

The weighted Weibull distribution (WWD) was developed by (Nasiru, 2015). It is said to be very flexible among other competing models. The cumulative density function (CDF) of the WWD is given by

$$F\left(x,\alpha,\gamma,\lambda\right)=1-e^{-\left(\gamma x^{\alpha}+\gamma\left(\lambda x\right)^{\alpha}\right)}, \tag{1}$$

where $x>0,\alpha>0,\gamma>0,\lambda>0$, α is a shape parameter, β and λ are scale parameters.

The corresponding probability density function (pdf) is obtained by differentiating the CDF in (1) and is given as

$$f\left(x,\alpha,\gamma,\lambda\right)=\alpha\gamma\left(1+\lambda^{\alpha}\right)x^{\alpha-1}e^{-\left(\gamma x^{\alpha}+\gamma\left(\lambda x\right)^{\alpha}\right)}\ . \tag{2}$$

The hazard function is defined as the ratio of the PDF to the survival function. This is presented as

$$H\left(x\right)=\frac{\alpha\gamma\left(1+\lambda^{\alpha}\right)x^{\alpha-1}e^{-\left(\gamma x^{\alpha}+\gamma\left(\lambda x\right)^{\alpha}\right)}}{e^{-\left(\gamma x^{\alpha}+\gamma\left(\lambda x\right)^{\alpha}\right)}}. \tag{3}$$

The quantile function which is very useful in generating random numbers from the distribution is obtained as

$$x\left(u\right)=\left[\frac{-\log\left(1-u\right)}{\gamma\left(1+\lambda^{\alpha}\right)}\right]^{1/\alpha}, \tag{4}$$

where u is the uniform distribution within the interval 0 and 1.

4 V-Mask

The CUSUM control chart is realized by plotting the sum $S_n=\sum_{i=1}^{n}\ln x_i$ versus the number of observations n. the V-mask is very important in determining the status of a system. The process is achieved by placing a V-mask on the final plotted CUSUM points in line with OS_1 or OS_{-1} parallel to the axis m. The points plotted earlier are then investigated to determine if they are found above or below the arms of the V-mask. If all the points fall within the two arms of the V-mask, then the process is judged to be in-control. On the other hand, if the past plotted points are outside the arms of the V-mask, then the process is assumed to be out of out-of-control.

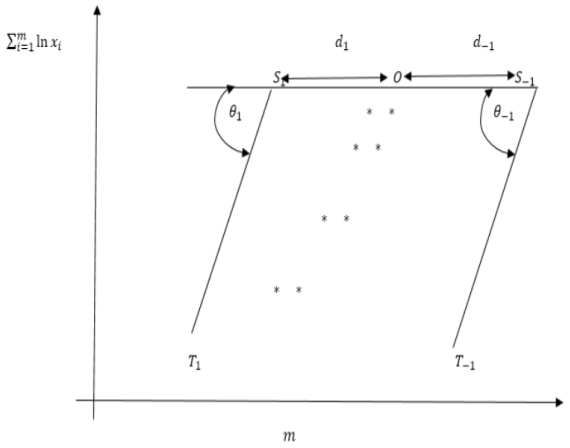

Fig. 1. V-mask

5 Cumulative Sum Control Chart of the WW Distribution

If $x_1, x_2, ..., x_n$ are randomly independent and identically distributed variables and follow the WWD, then the likelihood ratio for testing the hypotheses that there is a shift in γ and keeping other parameters fixed, is given as

$$H_0 : \gamma = \gamma_0$$

$$H_1 : \gamma = \gamma_1$$

Likelihood function for (2) when there is no shift in the scale parameters is

$$L_0 = \prod_{i=1}^{n}\left[\alpha\gamma_0\left(1+\lambda^{\alpha}\right)x^{\alpha-1}e^{-\left(\gamma_0 x^{\alpha}+\gamma_0(\lambda x)^{\alpha}\right)}\right]. \tag{5}$$

The likelihood function for a shift in the scale parameters is

$$L_1 = \prod_{i=1}^{n}\left[\alpha\gamma_1\left(1+\lambda^{\alpha}\right)x^{\alpha-1}e^{-\left(\gamma_1 x^{\alpha}+\gamma_1(\lambda x)^{\alpha}\right)}\right]. \tag{6}$$

The likelihood ratio $\left(L_R\right)$ of (5) and (6) is given as

$$L_R = \frac{\prod_{i=1}^{n}\left[\alpha\gamma_1\left(1+\lambda^{\alpha}\right)x^{\alpha-1}e^{-\left(\gamma_1 x^{\alpha}+\gamma_1(\lambda x)^{\alpha}\right)}\right]}{\prod_{i=1}^{n}\left[\alpha\gamma_0\left(1+\lambda^{\alpha}\right)x^{\alpha-1}e^{-\left(\gamma_0 x^{\alpha}+\gamma_0(\lambda x)^{\alpha}\right)}\right]}. \tag{7}$$

This is simplified as

$$L_R = \prod_{i=1}^{n}\left[\frac{\gamma_1}{\gamma_0}e^{-\left(\gamma_1 x^{\alpha}+\gamma_1(\lambda x)^{\alpha}\right)+\left(\gamma_0 x^{\alpha}+\gamma_0(\lambda x)^{\alpha}\right)}\right]. \tag{8}$$

Further simplification yields

$$L_R = \left(\frac{\gamma_1}{\gamma_0}\right)^n e^{-\left(\gamma_1 x^{\alpha}+\gamma_1\lambda^{\alpha}\sum_{i=1}^{n}x_i^{\alpha}\right)+\left(\gamma_0 x^{\alpha}+\gamma_0\lambda^{\alpha}\sum_{i=1}^{n}x_i^{\alpha}\right)}. \tag{9}$$

The continuation region of the SPTR differentiating between the two hypotheses is given by

$$\frac{\delta}{1-\theta} < L_R < \frac{1-\delta}{\theta},$$

where δ and θ are the types I and II errors. Substituting (9) in the continuation region gives

$$\frac{\delta}{1-\theta} < \left(\frac{\gamma_1}{\gamma_0}\right)^n e^{-\left(\gamma_1 x^{\alpha}+\gamma_1\lambda^{\alpha}\sum_{i=1}^{n}x_i^{\alpha}\right)+\left(\gamma_0 x^{\alpha}+\gamma_0\lambda^{\alpha}\sum_{i=1}^{n}x_i^{\alpha}\right)} < \frac{1-\delta}{\theta}. \tag{10}$$

Taking the natural logarithm of both sides gives

$$\log\left(\frac{\delta}{1-\theta}\right) < \left(\frac{\gamma_1}{\gamma_0}\right)^n e^{-\left(\gamma_1 x^\alpha + \gamma_1 \lambda^\alpha \sum_{i=1}^n x_i^\alpha\right) + \left(\gamma_0 x^\alpha + \gamma_0 \lambda^\alpha \sum_{i=1}^n x_i^\alpha\right)} < \log\left(\frac{1-\delta}{\theta}\right) . \tag{11}$$

If $\delta = 0$, then

$$n\log\left(\frac{\gamma_1}{\gamma_0}\right) - \left(\gamma_1 x^\alpha + \gamma_1 \lambda^\alpha \sum_{i=1}^n x_i^\alpha\right) + \left(\gamma_0 x^\alpha + \gamma_0 \lambda^\alpha \sum_{i=1}^n x_i^\alpha\right) < \log\left(\frac{1}{\theta}\right). \tag{12}$$

Factorizing yields

$$\sum_{i=1}^n x_i^\alpha \left(\gamma_0 \lambda^\alpha - \gamma_1 \lambda^\alpha + \gamma_0 - \gamma_1\right) < \log\left(\frac{1}{\theta}\right) - n\log\left(\frac{\gamma_1}{\gamma_0}\right). \tag{13}$$

simplifying gives

$$\sum_{i=1}^n x_i < \frac{{}^{1}\!/\!_{\alpha} \log\left(\frac{1}{\theta}\right) - n^{{}^{1}\!/\!_{\alpha}}\, {}^{1}\!/\!_{\alpha} \log\left(\frac{\gamma_1}{\gamma_0}\right)}{\left(\gamma_0 \lambda^\alpha - \gamma_1 \lambda^\alpha + \gamma_0 - \gamma_1\right)^{{}^{1}\!/\!_{\alpha}}}. \tag{14}$$

Writing (14) in the form $\sum_{i=1}^n x_i \le bx + q$, gives

$$\text{where } q = \frac{-{}^{1}\!/\!_{\alpha}\left(\log\left(\frac{1}{\theta}\right)\right)}{-\left[\lambda^\alpha\left(\gamma_0 - \gamma_1\right) - \left(\gamma_0 - \gamma_1\right)\right]^{{}^{1}\!/\!_{\alpha}}} \text{ and } b = \frac{n^{{}^{1}\!/\!_{\alpha}} \frac{1}{\alpha} \log\left(\frac{\gamma_1}{\gamma_0}\right)}{-\left[\lambda^\alpha\left(\gamma_0 - \gamma_1\right) + \left(\gamma_0 - \gamma_1\right)\right]^{{}^{1}\!/\!_{\alpha}}}.$$

The mark angle is obtained as

$$\theta = \tan^{-1}\left[\frac{\frac{1}{\alpha}\log\left(\frac{\gamma_1}{\gamma_0}\right)}{-\left[\lambda^\alpha\left(\gamma_0 - \gamma_1\right) + \left(\gamma_0 - \gamma_1\right)\right]^{{}^{1}\!/\!_{\alpha}}}\right].$$

5.1 Effects of right-side and left-side shifts in the value of gamma on the mask angle

Table 1 shows the effect of both right and left shifts in the value of gamma on the mask angle. The first part indicates the right shift and the second part shows the values of the left shift. The angle of the mask decreases in value when the shift in gamma is to the right. On the other hand, when there is a left shift in the value of gamma, the angle increases.

5.2 Effects of right-side and left-side shift in gamma on the lead distance

The lead distance of the V-mask is the distance between the last point plotted and the angle of the mask. It represents the maximum allowable deviations from the center line before a point is considered out of control. A larger lead distance shows: wider control limits, greater tolerance for variation, and reduced sensitivity to small shifts in the process. On the other hand, a smaller lead distance indicates a narrow control limit, less tolerance for variation, and increased sensitivity to small shifts in the process. It is by

$$|d| = \frac{-{}^{1}\!/\!_{\alpha}\left(\log\left(\frac{1}{\theta}\right)\right)}{-\left[\lambda^\alpha\left(\gamma_0 - \gamma_1\right) - \left(\gamma_0 - \gamma_1\right)\right]^{{}^{1}\!/\!_{\alpha}}}$$, where $\lambda_1 > \lambda_0$ and $\delta_1 > \delta_0$.

A right shift in the value of gamma causes the lead distance to decrease and a left shift in gamma leads to an increase in the value of the lead distance as indicated in the second part of Table 2.

Table 1. Effect of Right and left shift of gamma on the angle

γ_0	γ_1	α	λ	θ
0.001	0.01	2	5.0	78.5
0.001	0.05	2	5.0	56.9
0.001	0.09	2	5.0	44.2
0.001	0.12	2	5.0	37.7
0.001	0.18	2	5.0	29.2
0.001	0.23	2	5.0	24.5
0.001	0.29	2	5.0	20.7
0.001	0.31	2	5.0	19.6
0.001	0.36	2	5.0	17.5
0.001	0.40	2	5.0	16.1
γ_0	γ_1	α	λ	θ
0.1	0.2	2	5.0	7.6
0.1	0.13	2	5.0	9.5
0.1	0.09	2	5.0	11.5
0.1	0.05	2	5.0	14.9
0.1	0.02	2	5.0	21.2
0.1	0.015	2	5.0	23.2
0.1	0.007	2	5.0	28.8
0.1	0.005	2	5.0	31.2
0.1	0.003	2	5.0	34.8
0.1	0.001	2	5.0	41.8

Table 2. Effect of Right and left shift in gamma on the lead distance

γ_0	γ_1	λ	α	θ	d
0.1	0.4	0.01	0.2	0.03	97.1
0.1	0.7	0.01	0.2	0.03	48.5
0.1	1.0	0.01	0.2	0.03	32.4
0.1	1.3	0.01	0.2	0.03	24.3
0.1	1.8	0.01	0.2	0.03	17.1
0.1	2.3	0.01	0.2	0.03	13.2
0.1	2.9	0.01	0.2	0.03	10.4
0.1	3.4	0.01	0.2	0.03	8.8
0.1	3.6	0.01	0.2	0.03	8.3
0.1	4.0	0.01	0.2	0.03	7.5
γ_0	γ_1	λ	α	θ	d
4	3.9	12	0.1	2	- 245.7
4	3.4	12	0.1	2	- 41.0
4	3.0	12	0.1	2	- 24.6
4	2.6	12	0.1	2	- 17.6
4	2.1	12	0.1	2	- 12.9
4	1.7	12	0.1	2	- 10.7
4	1.3	12	0.1	2	- 9.1
4	0.8	12	0.1	2	- 7.7
4	0.3	12	0.1	2	- 6.6
4	0.09	12	0.1	2	- 6.3

An increase in the value of lambda from 0.01 to 12 with a right shift in gamma, increases the value of the lead distance and causes a decrease in lambda from 0,01 to 0.008 with a right-side shift in gamma, decreases the value of the lead distance as displayed in Table 3.

Table 3. Increase and decrease in the value of lambda with a right-side shift in gamma

γ_0	γ_1	λ	α	θ	d
0.1	0.4	10.0	0.2	0.03	- 99.9
0.1	0.7	10.0	0.2	0.03	- 50.0
0.1	1.0	10.0	0.2	0.03	- 33.3
0.1	1.3	10.0	0.2	0.03	- 25.0
0.1	1.8	10.0	0.2	0.03	- 17.6
0.1	2.3	10.0	0.2	0.03	- 13.6
0.1	2.9	10.0	0.2	0.03	- 10.7
0.1	3.4	10.0	0.2	0.03	- 9.1
0.1	3.6	10.0	0.2	0.03	- 8.6
0.1	4.0	10.0	0.2	0.03	- 7.7
γ_0	γ_1	λ	α	θ	d
0.1	0.4	0.008	0.2	0.03	94.4
0.1	0.7	0.008	0.2	0.03	47.2
0.1	1.0	0.008	0.2	0.03	31.5
0.1	1.3	0.008	0.2	0.03	23.6
0.1	1.3	0.008	0.2	0.03	23.6
0.1	1.8	0.008	0.2	0.03	16.7
0.1	2.3	0.008	0.2	0.03	12.9
0.1	2.9	0.008	0.2	0.03	10.1
0.1	3.4	0.008	0.2	0.03	8.6
0.1	3.6	0.008	0.2	0.03	8.1
0.1	4.0	0.008	0.2	0.03	7.3

However, both increases (0.01 to 10) and decreases (0.01 to 0.008) in lambda with either right side or left side shift in gamma have increasing effects on the value of the lead distance as shown in Table 4.

Table 4. Changes in the value of lambda with left and right shifts in gamma

γ_0	γ_1	λ	α	θ	d
4	3.9	10.0	0.1	2	- 198.4
4	3.4	10.0	0.1	2	- 33.1
4	3.0	10.0	0.1	2	- 19.8
4	2.6	10.0	0.1	2	- 14.2
4	2.1	10.0	0.1	2	- 10.4
4	1.7	10.0	0.1	2	- 8.6
4	1.3	10.0	0.1	2	- 7.3
4	0.8	10.0	0.1	2	- 6.2
4	0.3	10.0	0.1	2	- 5.4
4	0.09	10.0	0.1	2	- 5.0
γ_0	γ_1	λ	α	θ	d
4	3.9	0.008	0.1	2	- 396.9
4	3.4	0.008	0.1	2	- 66.2
4	3.0	0.008	0.1	2	- 39.7
4	2.6	0.008	0.1	2	- 28.4
4	2.1	0.008	0.1	2	- 20.9
4	1.7	0.008	0.1	2	- 17.3
4	1.3	0.008	0.1	2	- 14.7
4	0.8	0.008	0.1	2	- 12.4
4	0.3	0.008	0.1	2	- 10.7

Furthermore, both increases (0.1 to 0.9) or decreases (0.1 to 0.05) in the value of alpha with a right shift in gamma decrease the value of the lead distance The details are shown in Tables 5.

Table 5. Effect of changes in alpha with a right shift in gamma

γ_0	γ_1	λ	α	θ	d
0.1	0.4	0.01	0.9	0.03	13.2
0.1	0.7	0.01	0.9	0.03	6.6
0.1	1.0	0.01	0.9	0.03	4.4
0.1	1.3	0.01	0.9	0.03	3.3
0.1	1.8	0.01	0.9	0.03	2.3
0.1	2.3	0.01	0.9	0.03	1.8
0.1	2.9	0.01	0.9	0.03	1.4
0.1	3.4	0.01	0.9	0.03	1.2
0.1	3.6	0.01	0.9	0.03	1.1
0.1	4.0	0.01	0.9	0.03	1.0
γ_0	γ_1	λ	α	θ	d
0.1	0.4	0.01	0.05	0.03	1136.6
0.1	0.7	0.01	0.05	0.03	568.3
0.1	1.0	0.01	0.05	0.03	378.9
0.1	1.3	0.01	0.05	0.03	284.2
0.1	1.8	0.01	0.05	0.03	200.6
0.1	2.3	0.01	0.05	0.03	155.0
0.1	2.9	0.01	0.05	0.03	121.8
0.1	3.4	0.01	0.05	0.03	103.3
0.1	3.6	0.01	0.05	0.03	97.4
0.1	4.0	0.01	0.05	0.03	87.4

Again, both increase (0.1 to 0.9) and decrease (0.1 to 0.01) in alpha with a left-side shift in gamma increasing the value of the lead distance. The details are presented in Table 6.

Table 6. Effect of changes alpha with a left-side shift in gamma

γ_0	γ_1	λ	α	θ	d
4	3.9	20	0.9	2	- 0.92
4	3.4	20	0.9	2	- 0.15
4	3.0	20	0.9	2	- 0.09
4	2.6	20	0.9	2	- 0.07
4	2.1	20	0.9	2	- 0.05
4	1.7	20	0.9	2	- 0.04
4	1.3	20	0.9	2	- 0.03
4	0.8	20	0.9	2	- 0.03
4	0.3	20	0.9	2	- 0.02
4	0.09	20	0.9	2	- 0.02
γ_0	γ_1	λ	α	θ	d
4	3.9	12	0.01	2	- 27549.2
4	3.4	12	0.01	2	- 4591.5
4	3.0	12	0.01	2	- 2754.9
4	2.6	12	0.01	2	- 1967.8
4	2.1	12	0.01	2	- 1450.0
4	1.7	12	0.01	2	- 1197.8
4	1.3	12	0.01	2	- 1020.3
4	0.8	12	0.01	2	- 860.9
4	0.3	12	0.01	2	- 744.6
4	0.09	12	0.01	2	- 704.6

Moreover, an increase (2 to 9) and decrease (2 to 0.5) in the value of theta with a right-side shift in gamma decreases the lead distance as detailed in Table 7.

Table 7. Effect on changes in theta with a right-side shift in gamma

γ_0	γ_1	λ	α	θ	d
0.1	0.4	0.01	0.2	9	33.3
0.1	0.7	0.01	0.2	9	16.7
0.1	1.0	0.01	0.2	9	11.1
0.1	1.3	0.01	0.2	9	8.3
0.1	1.8	0.01	0.2	9	5.9
0.1	2.3	0.01	0.2	9	4.5
0.1	2.9	0.01	0.2	9	3.6
0.1	3.4	0.01	0.2	9	3.0
0.1	3.6	0.01	0.2	9	2.9
0.1	4.0	0.01	0.2	9	2.6
γ_0	γ_1	λ	α	θ	d
0.1	0.4	0.01	0.2	0.5	127.5
0.1	0.7	0.01	0.2	0.5	63.8
0.1	1.0	0.01	0.2	0.5	42.5
0.1	1.3	0.01	0.2	0.5	31.9
0.1	1.8	0.01	0.2	0.5	22.5
0.1	2.3	0.01	0.2	0.5	17.4
0.1	2.9	0.01	0.2	0.5	13.7
0.1	3.4	0.01	0.2	0.5	11.6
0.1	3.6	0.01	0.2	0.5	10.9
0.1	4.0	0.01	0.2	0.5	9.8

Another observation is that an increase (2 to 9) in the value of theta with a left-side shift in the value of gamma increases the value of the lead distance. On the other hand, a decrease (2 to 0.5) in the value of theta with a left-side shift in the value of gamma decreases the value of the lead distance as indicated in Table 8.

Table 8. Effect of changes in theta with a left-side shift in gamma

γ_0	γ_1	λ	α	θ	d
4	3.9	12	0.1	9	- 778.9
4	3.4	12	0.1	9	- 129.8
4	3.0	12	0.1	9	- 77.9
4	2.6	12	0.1	9	- 55.6
4	2.1	12	0.1	9	- 41.0
4	1.7	12	0.1	9	- 33.9
4	1.3	12	0.1	9	- 28.8
4	0.8	12	0.1	9	- 24.3
4	0.3	12	0.1	9	- 21.1
4	0.09	12	0.1	9	- 19.9
γ_0	γ_1	λ	α	θ	d
4	3.9	12	0.1	0.5	245.7
4	3.4	12	0.1	0.5	41.0
4	3.0	12	0.1	0.5	24.6
4	2.6	12	0.1	0.5	17.6
4	2.1	12	0.1	0.5	12.9
4	1.7	12	0.1	0.5	10.7
4	1.3	12	0.1	0.5	9.1
4	0.8	12	0.1	0.5	7.7
4	0.3	12	0.1	0.5	6.6
4	0.09	12	0.1	0.5	6.3

6 Average Run Length

Average Run length (ARL) is the average number of samples or observations taken before a control chart signals an out-of-control condition. It measures the effectiveness of a control chart in detecting process shifts. A smaller ARL indicates faster detection of a process shift and also shows a reduced time to signal an out-of-control condition. The ARL is affected by: sample size, control limits, process variability, shift size, and chart type. The ARL is given by

$$ARL = \frac{-\ln \alpha}{E[Z]}.$$

where $Z = \frac{f_1(x, \alpha, \gamma_1, \lambda)}{f_0(x, \alpha, \gamma_0, \lambda)}$.

Using the PDF given in (1) then

$$Z = \frac{\alpha\gamma_1\left(1+\lambda^{\alpha}\right)x^{\alpha-1}e^{-\left(\gamma_1 x^{\alpha}+\gamma_1(\lambda x)^{\alpha}\right)}}{\alpha\gamma_0\left(1+\lambda^{\alpha}\right)x^{\alpha-1}e^{-\left(\gamma_0 x^{\alpha}+\gamma_0(\lambda x)^{\alpha}\right)}}. \tag{15}$$

This is simplified as

$$Z = \frac{\gamma_1}{\gamma_0}e^{\left(\gamma_0 x^{\alpha}+\gamma_0(\lambda x)^{\alpha}\right)-\left(\gamma_1 x^{\alpha}+\gamma_1(\lambda x)^{\alpha}\right)}. \tag{16}$$

Taking the natural logarithm of (16) yields

$$\ln Z = \ln\left[\frac{\gamma_1}{\gamma_0}e^{\left(\gamma_0 x^{\alpha}+\gamma_0(\lambda x)^{\alpha}\right)-\left(\gamma_1 x^{\alpha}+\gamma_1(\lambda x)^{\alpha}\right)}\right]. \tag{17}$$

Taking expectation of both sides gives

$$E[\ln Z] = \ln\left(\frac{\gamma_1}{\gamma_0}\right)\left(\gamma_0 E[x]^{\alpha}+\gamma_0\left(\lambda E[x]\right)^{\alpha}\right)-\left(\gamma_1 E[x]^{\alpha}+\gamma_1\left(\lambda E[x]\right)^{\alpha}\right). \tag{18}$$

Simplifying further gives

$$E[\ln Z] = \ln\left(\frac{\gamma_1}{\gamma_0}\right)+\gamma_0-\gamma_1+\left(\gamma_0\lambda^{\alpha}-\gamma_1\lambda^{\alpha}\right)E[x]^{\alpha}.$$

(19)

By definition,

$$E[x] = \int_{\gamma}^{\infty} xf(x, \alpha, \gamma, \lambda)dx.$$

Substituting (2) into the integral yields

$$E[x] = \alpha\gamma\left(1+\lambda^{\alpha}\right)\int_{\gamma}^{\infty} x^{\alpha} e^{-\left(\gamma x^{\alpha}+\gamma(\lambda x)^{\alpha}\right)} dx .$$

Let $u = \gamma x^{\alpha} + \gamma(\lambda x)^{\alpha}$ then $x = \left(\frac{u}{\gamma+\gamma\lambda^{\alpha}}\right)^{1/\alpha}$, if $x = 1$ then $u = \gamma\left(1+\lambda^{\alpha}\right)$ and if $x = \infty$ then $u = \infty$.

Also $\frac{du}{dx} = \alpha\gamma x^{\alpha-1} + \alpha\gamma\lambda^{\alpha} x^{\alpha-1}$, and $dx = \frac{du}{\alpha\gamma x^{\alpha-1} + \alpha\gamma\lambda^{\alpha} x^{\alpha-1}}$.

This implies

$$E[x] = \alpha\gamma\left(1+\lambda^{\alpha}\right)\int_{\gamma\left(1+\lambda^{\alpha}\right)}^{\infty} ue^{-u}\frac{du}{\alpha\gamma\left(1+\lambda^{\alpha}\right)x^{\alpha-1}} .$$

Simplifying gives

$$E[x] = \left(\gamma+\gamma\lambda^{\alpha}\right)^{-1/\alpha}\int_{\gamma\left(1+\lambda^{\alpha}\right)}^{\infty} u^{\frac{1+\alpha}{\alpha}-1} e^{-u} du ,$$

And

$$E[x] = \left(\gamma+\gamma\lambda^{\alpha}\right)^{-1/\alpha}\Gamma\left(\tfrac{1+\alpha}{\alpha}, \gamma\left(1+\lambda^{\alpha}\right)\right).$$

Substituting the expression for $E[x]$ into (20) produces

$$E[\ln Z] = \ln\left(\frac{\gamma_1}{\gamma_0}\right) + \gamma_0 - \gamma_1 + \left(\gamma_0\lambda^{\alpha} - \gamma_1\lambda^{\alpha}\right)\left[\left(\gamma+\gamma\lambda^{\alpha}\right)^{-1/\alpha}\Gamma\left(\tfrac{1+\alpha}{\alpha}, \gamma\left(1+\lambda^{\alpha}\right)\right)\right]^{\alpha} . \tag{20}$$

Simplify further gives

$$E[\ln Z] = \ln\left(\frac{\gamma_1}{\gamma_0}\right) + \gamma_0 - \gamma_1 + \left(\gamma_0\lambda^{\alpha} - \gamma_1\lambda^{\alpha}\right)\frac{\Gamma\left(\tfrac{1+\alpha}{\alpha}, \gamma\left(1+\lambda^{\alpha}\right)\right)^{\alpha}}{\gamma+\gamma\lambda^{\alpha}} .$$

The ARL is finally expressed as

$$ARL = \frac{-\ln\alpha}{\ln\left(\frac{\gamma_1}{\gamma_0}\right) + \gamma_0 - \gamma_1 + \left(\gamma_0\lambda^{\alpha} - \gamma_1\lambda^{\alpha}\right)\frac{\Gamma\left(\tfrac{1+\alpha}{\alpha}, \gamma\left(1+\lambda^{\alpha}\right)\right)^{\alpha}}{\gamma+\gamma\lambda^{\alpha}}} . \tag{21}$$

Right-side changes in gamma value increase the value of the ARL whereas a left-side shift in gamma decreases ARL. The details are shown in Table 9.

The ARL also increases in value when lambda is increased (2 to 4.1) with a right-side shift in gamma. And decreases in value with a left-side shift in gamma as displayed in Table 10.

A decrease (2 to 0.5) in the value of lambda with a right-side shift in the value of gamma increases the value of the ALR whereas the same decrease in lambda with a left-side shift in the value of gamma produces a decreasing ARL. The details are shown in Table 11.

Both increase (0.1 to 0.9) and decrease (0.1 to 0.01) in alpha, with a right-side shift in gamma slowly increasing the value of the ARL as detailed in Table 12.

Table 9. Effect of right and left sides shifts in gamma on the ARL

γ_0	γ_1	γ	λ	α	**ARL**
7	12	3	2	0.1	- 1.9891
7	13.5	3	2	0.1	- 1.5248
7	14.6	3	2	0.1	- 1.3013
7	16.5	3	2	0.1	- 1.0376
7	17.5	3	2	0.1	- 0.9374
7	19.0	3	2	0.1	- 0.8185
7	21.4	3	2	0.1	- 0.6802
7	22.5	3	2	0.1	- 0.6312
7	25.8	3	2	0.1	- 0.5189
7	27.1	3	2	0.1	- 0.4660
γ_0	γ_1	γ	λ	α	ARL
7	6.85	3	2	0.1	67.5629
7	6.2	3	2	0.1	12.7162
7	5.9	3	2	0.1	9.2660
7	5.4	3	2	0.1	6.3930
7	5.1	3	2	0.1	4.4731
7	4.7	3	2	0.1	3.8251
7	4.3	3	2	0.1	3.3461
7	3.9	3	2	0.1	2.9784
7	3.5	3	2	0.1	2.6254
7	3.0	3	2	0.1	2.2648
7	2.3	3	2	0.1	2.1089

Table 10. Increase in the value of lambda with right and left shifts in gamma

γ_0	γ_1	γ	λ	α	**ARL**
7	12	3	4.1	0.1	- 1.9850
7	13.5	3	4.1	0.1	- 1.5219
7	14.6	3	4.1	0.1	- 1.2989
7	16.5	3	4.1	0.1	- 1.0359
7	17.5	3	4.1	0.1	- 0.9359
7	19.0	3	4.1	0.1	- 0.8173
7	21.4	3	4.1	0.1	- 0.6792
7	22.5	3	4.1	0.1	- 0.6303
7	25.8	3	4.1	0.1	- 0.5182
7	27.1	3	4.1	0.1	- 0.4842
γ_0	γ_1	γ	λ	α	ARL
7	6.85	3	4.1	0.1	67.3758
7	6.2	3	4.1	0.1	12.6790
7	5.9	3	4.1	0.1	9.2383
7	5.4	3	4.1	0.1	6.3729
7	5.1	3	4.1	0.1	5.3789
7	4.7	3	4.1	0.1	4.4580
7	4.3	3	4.1	0.1	3.8116
7	3.9	3	4.1	0.1	3.3337

7	3.5	3	4.1	0.1	2.9668
7	3.0	3	4.1	0.1	2.6144
7	2.3	3	4.1	0.1	2.2541

Table 11. Effect of decrease in lambda with right and left shifts in gamma

γ_0	γ_1	γ	λ	α	**ARL**
7	12	3	0.5	0.1	- 1.9970
7	13.5	3	0.5	0.1	- 1.5305
7	14.6	3	0.5	0.1	- 1.3059
7	16.5	3	0.5	0.1	- 1.0410
7	17.5	3	0.5	0.1	- 0.9404
7	19.0	3	0.5	0.1	- 0.8210
7	21.4	3	0.5	0.1	- 0.6821
7	22.5	3	0.5	0.1	- 0.6329
7	25.8	3	0.5	0.1	- 0.5202
7	27.1	3	0.5	0.1	- 0.4860
γ_0	γ_1	γ	λ	α	ARL
7	6.85	3	0.5	0.1	67.9282
7	6.2	3	0.5	0.1	12.7887
7	5.9	3	0.5	0.1	9.3203
7	5.4	3	0.5	0.1	6.4322
7	5.1	3	0.5	0.1	5.4303
7	4.7	3	0.5	0.1	4.5026
7	4.3	3	0.5	0.1	3.8515
7	3.9	3	0.5	0.1	3.3703
7	3.5	3	0.5	0.1	3.0012
7	3.0	3	0.5	0.1	2.6471
7	2.3	3	0.5	0.1	2.2860

Table 12. Increase in alpha with a right-side shift in gamma

γ_0	γ_1	γ	λ	α	ARL
7	12.0	3	2	0.9	- 1.0795
7	13.5	3	2	0.9	- 0.8284
7	14.6	3	2	0.9	- 0.7074
7	16.5	3	2	0.9	- 0.5646
7	17.5	3	2	0.9	- 0.5103
7	19.0	3	2	0.9	- 0.4458
7	21.4	3	2	0.9	- 0.3708
7	22.5	3	2	0.9	- 0.3442
7	25.8	3	2	0.9	- 0.2832
7	27.1	3	2	0.9	- 0.2647
7	27.9	3	2	0.9	- 0.2544
γ_0	γ_1	γ	λ	α	ARL
7	12.0	3	2	0.01	- 3.0122
7	13.5	3	2	0.01	- 2.3089
7	14.6	3	2	0.01	- 1.9702
7	16.5	3	2	0.01	- 1.5709
7	17.5	3	2	0.01	- 1.4190
7	19.0	3	2	0.01	- 1.2390
7	21.4	3	2	0.01	- 1.0295
7	22.5	3	2	0.01	- 0.9553
7	25.8	3	2	0.01	- 0.7852
7	27.1	3	2	0.01	- 0.7337
7	27.9	3	2	0.01	- 0.7052

The ARL also decreases in value when alpha is increased (0.1 to 0.9) and decreases (0.1 to 0.01) with a left-side shift in gamma as shown in Table 13.

Table 13. Increase in alpha with a left-side shift in gamma

γ_0	γ_1	γ	λ	α	ARL
7	6.85	3	2	0.9	36.4686
7	6.2	3	2	0.9	6.8562
7	5.9	3	2	0.9	4.9932
7	5.4	3	2	0.9	3.4414
7	5.1	3	2	0.9	2.9028
7	4.7	3	2	0.9	2.4038
7	4.3	3	2	0.9	2.0532
7	3.9	3	2	0.9	1.7938
7	3.5	3	2	0.9	1.5944
7	3.0	3	2	0.9	1.4023
7	2.3	3	2	0.9	1.2048
γ_0	γ_1	γ	λ	α	ARL
7	6.85	3	2	0.01	102.3800
7	6.2	3	2	0.01	19.2717
7	5.9	3	2	0.01	14.0439
7	5.4	3	2	0.01	9.6907
7	5.1	3	2	0.01	8.1804
7	4.7	3	2	0.01	6.7818
7	4.3	3	2	0.01	5.8001
7	3.9	3	2	0.01	5.0745
7	3.5	3	2	0.01	4.5178
7	3.0	3	2	0.01	3.9834
7	2.3	3	2	0.01	3.4380

7 Practical Demonstration

In this section, the developed CUSUM chart is evaluated with random numbers generated from the distribution and real dataset from the world of work.

Table 14. Practical illustration with random numbers

x	**Log (x)**	**CUSUM**
5.1259	1.6343	1.6
2816.6450	7.9433	9.5
227.9300	5.4249	14.9
17.6351	2.8699	17.8
296.9666	5.6902	23.5
145.8691	4.9827	28.5
681.4453	6.5242	35.0
986.7509	6.8944	41.9
338.4893	5.8245	47.7
107.6000	4.6784	52.4
1441.1070	7.2732	59.7
18.5188	2.9187	62.6
33.1530	3.5011	66.1
216.8271	5.3791	71.5
435.9000	6.0774	77.6
11.9293	2.4790	80.1
102.3200	4.6281	84.7

43.4645	3.7719	88.5
9.5314	2.2544	90.8
77462.2400	11.2575	102.1

7.1 Random sample from the WW distribution

A random sample of size of twenty (20) was drawn from the WWD using the quantile function given in (4) and the values are shown in Table 14.

Fig. 2 displays the CUSUM plot of these random numbers. It shows only three points are in control, and the rest of the plotted points are outside the left area of the V-mask. It does show the sensitivity of the WWD CUSM control chart over the Shewhart chart.

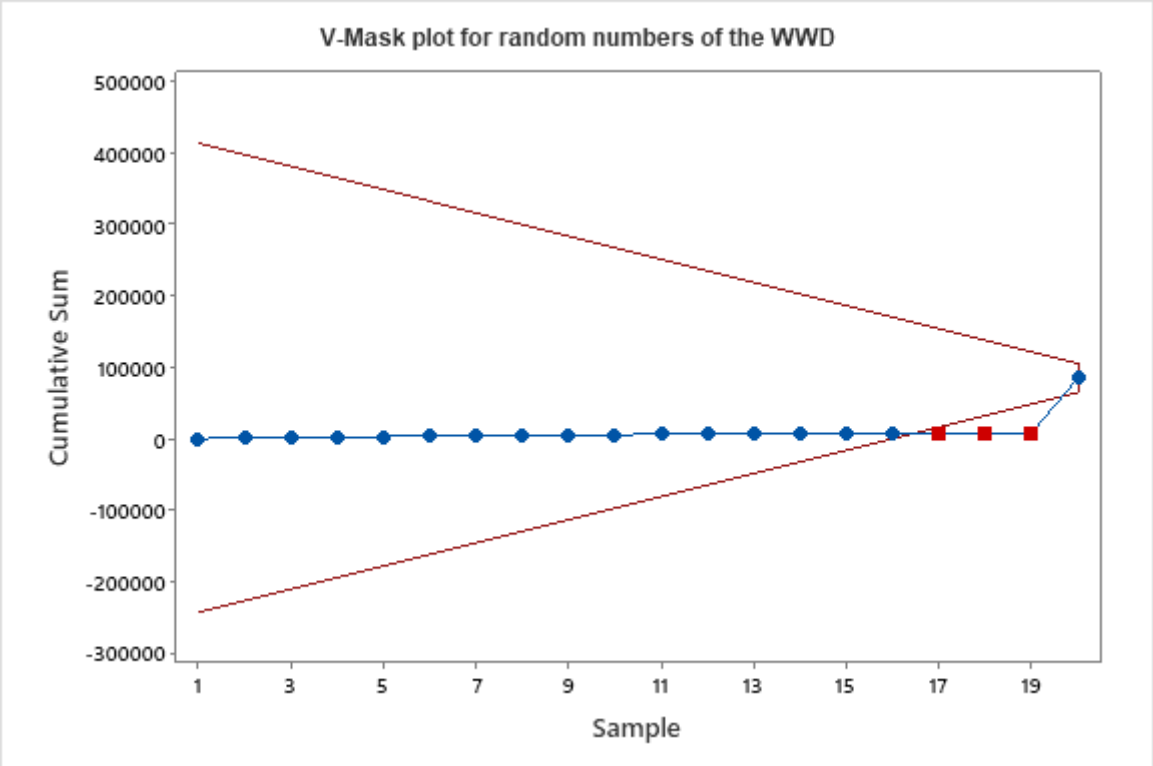

Fig. 2. V-mask CUSUM of the WWD random numbers

7.2 Temperature dataset

The second dataset is obtained from the Kabsad Scientific Hospital in the Tamale Metropolis in the Northern region of Ghana. The data represents the temperature values of some thirty (30) selected patients in the outpatient department for September 2024. The observations are as follows:

37.1, 36.9, 36.4, 36.1, 36.4, 36.6, 35.6, 37.0, 36.7, 36.7, 36.2, 36.0, 36.8, 36.6,36.6, 36.0, 36.7, 36.7, 37.1, 36.4, 36.2, 36.8, 36.5, 37.3, 37.5, 36.3, 36.4, 36.7, 36.2, 36.6.

Fig. 3 shows the mean plot of the temperature dataset and the graph indicates the system is in control since no value is plotted outside the control limits. This means that no action is needed to be taken by management.

The V-mask plot of the same temperature dataset is shown in Fig. 4. It indicates only one point is in control and the rest of the plotted points are located outside the control limits. This shows the sensitivity of the CUSUM in detecting smaller shifts in a process system than the Shewhart control charts. The details are shown in Fig. 4. An

out-of-control point on a health monitoring chart can have significant implications for patient care, quality of care, and healthcare outcomes.

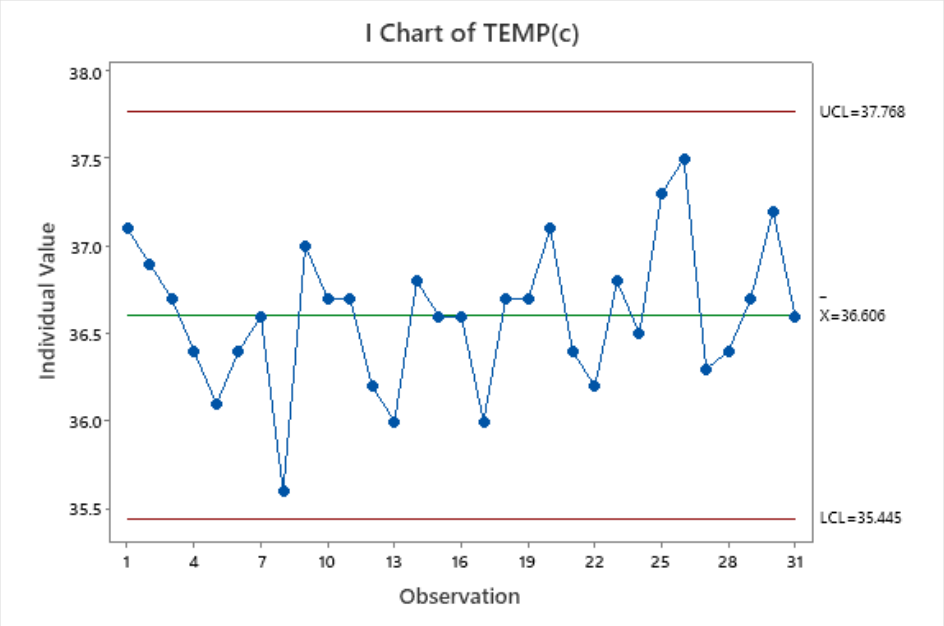

Fig. 3. Shewhart control Chart for the temperature dataset

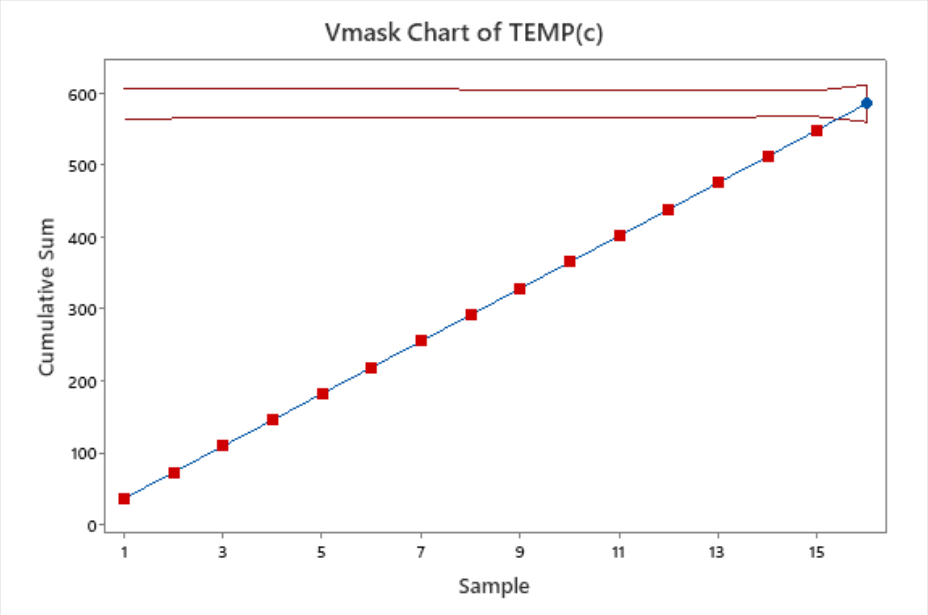

Fig. 4. V-mask plot of the temperature dataset

8 Conclusion

The right-side shift in the size of gamma decreases the size of the mask angle whereas the left-side shift in gamma increases the size of the mask angle. The right-side shift in the value of gamma reduces the lead distance and the left-side shift in gamma increases the size of the lead distance. If there is a right-side shift in gamma and lambda, the lead distance increases and a right-side shift in gamma with a decrease in the lambda value decreases the lead distance. Again, a left-side shift in gamma with an increase or decrease in the lambda value increases the lead distance's value. Also, an increase or decrease in alpha value decreases the value of lead distance when there is a right-side shift in gamma. On the other hand, an increase or decrease in the alpha value with a left-side shift in gamma increases the value of the lead distance. Both increase or decrease in the value of

theta with a right-side shift decreases the value of the lead distance. An increase in the value of theta with a left-side shift in gamma increases the value of the lead distance and a decrease in theta with a left-side shift in gamma decreases the value of the lead distance. Not all but also a right-side shift in gamma increases the value of the average run length and a left-side shift in gamma decreases the value of the average run length. An increase or a decrease in lambda with a right-side shift in gamma increases the value of the average run length. Similarly, an increase or decrease in the value of lambda with a left-side shift decreases the value of the average run length. Both increase or decrease in the value of alpha increases in the average run length. Last but not least, an increase or a decrease in the alpha with a left-side shift in gamma decreases the average run length. The practical demonstration indicates that the proposed constructed cumulative sum control chart is sensitive to detecting a slight shift in a process system. An out-of-control point on a health monitoring chart can have significant implications for patient care, quality of care, and healthcare outcomes. Other impacts are delayed or inadequate treatment, increased morbidity and mortality, decreased quality of life, increased healthcare costs, and reduced patient satisfaction.

Disclaimer (Artificial Intelligence)

We the authors, hereby declare that NO generative AI technologies such as Large Language Models (ChatGPT, COPILOT, etc) and text-to-image generators have been used during writing or editing of this manuscript.

Competing Interests

We the authors have declared that no competing interests exist.

References

Abass, N. (2023). On efficient change point detection using a step CUSUM control chart. *Quality Engineering*, 35(4): 712-728.

Aslam, M., Shafqat, A. and Albassam, M. (2024). A new CUSUM control chart under uncertainty with applications in petroleum and meteorology. *PLOS ONE*. 16(2): e0246185.

Champ, C. W. and Woodall, W. H. (2001). Exact results for Shewhart control charts with supplementary run rules. *Technometrics*, 43(4): 462-469.

Chaudhary, A. M., Sanaullah, A., Hanif, M., Almazah, M. M. A., Albasheir, N. A., & Al-Duais, F. S. (2023). Efficient Monitoring of a Parameter of Non-Normal Process Using a Robust Efficient Control Chart: A Comparative Study. *Mathematics*, *11*(19), 4157. https://doi.org/10.3390/math11194157

Devore, J. L. (2012). Probability and statistics for engineering and the sciences (8th edition). *Brooks/Cole Cengage Learning*. ISBN-13:978-0-538-73352-6.

Doganaksoy, N. and Hahn, G. J. (2020). How to use a CUSUM chart for process improvement. *Quality Progress*, 53(6): 34-41.

Grigg, O. A., and Farewell, V. T. (2020). Cumulative sum analysis: a simple and practical tool for monitoring and improvement. *Journal of Quality Technology*, 52(2): 133-146.

Hawkins, D. M. (1993). Cumulative sum control charting: an overview. *Quality and Reliability Engineering International*, 9(2): 161-171.

Hu, Zhang, S., Zhang, J., Saghir, A. (2023). Efficient CUSUM control charts for monitoring the multivariate coefficient of variation. *Computers and Industrial Engineering*. 197.109159.

Khalil, U., Khan, T. S., Hamid, W. A., Khan, D. M. and Hamiraz, M. (2024). A robust CUSUM control chart for median absolute deviation baed on trimming and winsorization. PLOS ONE, 19(5): e0297544.

Lucas, J. M. (1982). Combined Shewhart-CUSUM quality control schemes. *Journal of Quality Technology*, 14(2): 51-59.

Luguterah, A. (2015). Unified cumulative sum control chart for monitoring shifts in the parameters of the Erlang-Truncated exponential distribution. *Far East Journal of Theoretical Statistics*, 50(1): 65-76.

Nasiru, S. (2015). Another weighted Weibull distribution from Azzalini's family. *European Scientific Journal*, 11(9). ISSN: 1857-7881 (Print) e-ISSN 1857-7431.

Nasiru, S. (2016). One-sided cumulative sum control chart for monitoring shifts in the shape parameter of Pareto distribution. *International Journal of Productivity and Quality Management*, 19(2): 160.

Nazir, H. Z., Ikram, M., Amir, M. W., Akhtar, N., Ababas, Z. and Riaz, M. (2024). Proper choice of location CUSUM control charts for different environment. *Quality and Reliability Engineering International*, 40(6): 3537-3554.

Page, E. S. (1954). Continuous inspection schemes, *Biometrika*, 41(1/2): 100-115

Rao, G. S. (2013). One-side cumulative sum control chart for the Erlang-Truncated exponential distribution. *CMST*, 19(4): 229-234.

Sayibu, S. B. and Luguterah, A. (2018). Two-sided cumulative sum control chart for monitoring shifts in the shape parameter of the Pareto distribution. *Journal of Statistics and Applied Probability*, 7(1): 29-37.

Sayibu, S. B. and Maahi, T. (2017). Unified sum control chart for monitoring shifts in the parameters of the Pareto distribution. *International Journal of Statistics and Applications*, 7(3): 170-177.

Sayibu, S. B., Jabir, H. and Abdul-Salam, S. (2017). One-sided cumulative sum control chart for monitoring shift in the scale parameter delta, of the new Weibull-Pareto distribution. *International Journal of Probability and Statistics*, 6(4): 76-81.

Woodall, W. H. and Adams, B. M. (1993). The statistical design of CUSUM charts. *Quality Engineering*, 5(4): 559-570.

Xie, M. and Goh, T. N. (2022). CGR-CUSUM: a continuous time generalized rapid response cumulative sum. *Quality and Reliability Engineering*, 38(3): 537-548.

Zhang, Y. and Woodall, W. H. (2019). Distribution-free cumulative sum control charts using bootstrap-based control limits. *Quality and Reliability Engineering International*, 35(6): 142-1433.

Peer-review history:
The peer review history for this paper can be accessed here (Please copy paste the total link in your browser address bar)
https://www.sdiarticle5.com/review-history/128079